# Conducting High-Spin ($S$ = 1) Organic Diradical with Robust Stability

Shuyang Zhang[†], Maren Pink[#], Tobias Junghoefer[§], Wenchao Zhao[⊥], Sheng-Ning Hsu[⊥], Suchada Rajca[†], Bryan W. Boudouris[⊥,‡], Maria Benedetta Casu*[§], and Andrzej Rajca*[†]

[†]Department of Chemistry, University of Nebraska, Lincoln, Nebraska 68588-0304, United States.

[#]IUMSC, Department of Chemistry, Indiana University, Bloomington, Indiana 47405-7102, United States.

[§]Institute of Physical and Theoretical Chemistry, University of Tübingen, 72076 Tübingen, Germany.

[⊥] Charles D. Davidson School of Chemical Engineering and [‡] Department of Chemistry, Purdue University, West Lafayette, IN 47907

**ABSTRACT:** Triplet ground-state organic molecules are of interest with respect to several emerging technologies but usually show limited stability, especially, as thin films. We report an organic diradical, based entirely on two Blatter radicals, that possesses triplet ground state ($2J/k \approx 220$ K, $\Delta E_{ST} \approx 0.4$ kcal mol$^{-1}$) and robust stability, with onset of decomposition above 264 °C (TGA). Polycrystalline diradical is a good electrical conductor with conductivity comparable to the out-of-plane conductivity in highly oriented pyrolytic graphite (HOPG). The diradical is evaporated under ultra-high vacuum to form thin films, which are stable on air for at least 18 and 48 h, as demonstrated by X-ray photoelectron and electron paramagnetic resonance (EPR) spectroscopies, respectively.

The recently reported high spin organic diradicals **1** and **2** have attracted a great interest due to their remarkable thermal stability that permits vapor-based growth of thin films under high- or ultra-high vacuum (UHV).[1,2] The design of the diradicals is based on the 1,2,4-benzotriazinyl (Blatter) radical substituted with a nitronyl nitroxide (NN) radical, taking advantage of the Blatter monoradical's high thermal stability and the NN low molecular weights to facilitate evaporation. However, **1** and **2** possess limited stability with onset of decomposition <180 °C (thermogravimetric analysis, TGA), and consequently, the diradical thin films, in particular of **2**, undergo rapid decomposition in air.[2]

We consider a diradical based entirely on the Blatter radical building block, to fully take advantage of its excellent thermal stability.[3,4] A huge challenge is in the design and synthesis of such diradicals. There are a few molecules that formally incorporate two Blatter radicals reported to date, e.g., zwitterionic TetraPhenylHexaazaAnthracene (TPHA), *ortho*-DiBlatterTrimethylenemethane (*o*-DBT) or Chichibabin-type diradicaloid **3**.[5,6] These molecules exclusively possess low-spin ($S = 0$) ground states. This is not surprising. According to the Ovchinnikov parity models, TPHA, **3**, and its biphenyl isomers are predicted to possess $S = 0$ ground states, because of the absence of significant spin sign alternation at the atoms connecting two radicals.[7,8] Although the alternating spin connectivity in *o*-DBT predicts the $S = 1$ ground state, severe out-of-plane twisting is well-known to lead to an $S = 0$ ground state.[9]

Examination of the parity models and spin density distribution in the parent Blatter radical leads us to note that a connection at the C3 and C7 position would provide a high-spin diradical (Figure 1). We design the di-Blatter diradical **4** by taking advantage of the negative spin density at C3 within the Blatter radical moiety (green dot, Figure 1). A *tert*-butyl group at the site of the largest spin density in the annelated benzene ring[1] would enhance stability and solubility of the diradical.

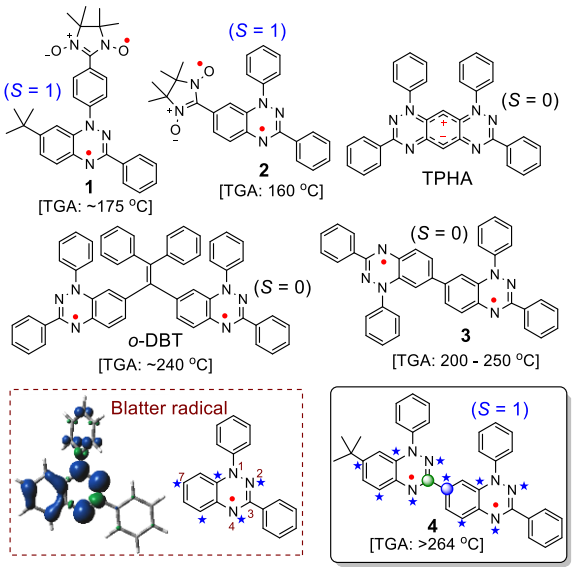


**Figure 1.** Blatter-based diradicals: TGA onset of decomposition ≈ 1% mass loss. Blatter radical and its spin density map at the UB3LYP/6-31G(d,p) level of theory; positive (blue) and negative (green) spin densities are shown at the isodensity level of 0.002 electron/Bohr.

We set out to explore the synthesis of di-Blatter diradical and faced a tremendous challenge with various unsuccessful convergent synthetic approaches. The breakthrough was achieved after extensive attempts using a divergent route, in which two benzotriazinyl rings are formed in one synthetic step (Scheme 1).

Here we report the synthesis, characterization and thin-film preparation of di-Blatter diradical **4**. The diradical possesses a triplet ground state and robust thermal stability, with an onset of decomposition above 264 °C – the highest temperature among high-spin diradicals studied by TGA. Remarkably,

crystalline **4** exhibits electrical conductivity, with an outstanding $\sigma \approx 0.01$ S cm$^{-1}$ at room temperature and $\sigma \sim 10$ S cm$^{-1}$ in the $T = 294$ –110 K range, as measured by a two-probe method and estimated by EPR spectroscopy, respectively. This value of $\sigma$ may be compared to typical neutral π-radicals that are insulators with $\sigma < 10^{-10}$ S cm$^{-1}$ or to recent reports of nitroxide-based glassy polymer with $\sigma \approx 0.3$ S cm$^{-1}$, or bis(thiazolyl)-related radicals with $\sigma \approx 0.04$ S cm$^{-1}$, or bis(phenalenyl) radicals with $\sigma \approx 0.3$ S cm$^{-1}$.[10,11] The diradical can be evaporated under UHV to obtain thin films of **4** on silicon substrates, which remain unchanged after exposure to air for at least 18 – 48 h.

The synthesis of **4** starts with the copper-catalyzed C-N bond coupling reaction of **5** with methyl 4-amino-3-iodo-benzoate to produce **6**. The ester group in **6** is hydrolyzed and the resultant carboxylic acid **7** is activated with 1,1'-carbonyldiimidazole (CDI), followed by the reaction with phenylhydrazine. The resultant synthetic intermediate **8** is subjected to a C-N bond coupling reaction with 4-*tert*-butyl-2-iodo-aniline to provide compound **9**. Acid-catalyzed double cyclization of **9** is followed by air oxidation under basic conditions to produce diradical **4** in about 50% isolated yield. Notably, when the cyclization step is carried out for 24 h, instead of 2 h, an approximately equimolar mixture of diradical **4** and by-product monoradical **10** is isolated (Scheme 1).[12]

**Scheme 1.** Synthesis of diradical **4** and monoradical **10**.

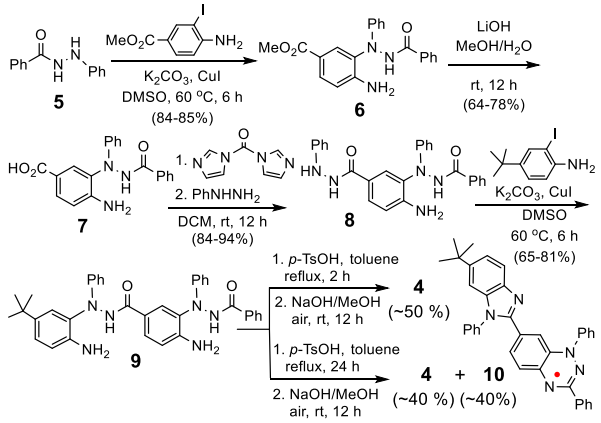


Structures of **4** and **10** are confirmed by X-ray crystallography (Figure 2 and SI). In diradical **4**, two fused-ring Blatter radical moieties are nearly coplanar, as indicated by the mean deviation from plane of 0.0719 Å for the plane defined by the N1-N6 and C1-C20 atoms. Also, the dihedral angle along the C4-C5 bond is 8.20 (0.12)°.[13] Thus, the conformation adopted by **4** in the crystal is near optimum for attaining both strong ferromagnetic coupling and electrical conductivity. Molecules of **4** form one-dimensional (1-D) π-stacks along the crystallographic *a*-axis, which coincides with the longest dimension of the single crystal plate/needle (Figure 2C), with average plane-to-plane distance of 3.482 Å (planes defined by the N1-N6 and C1-C20 atoms). In addition to a short C10···C12 = 3.381 Å contact within the 1-D π-stack, there are multiple C···C and N···C contacts within the sum of van der Waals radii plus 0.1 Å distances (Figs. S1 and S3, SI). Because most of these contacts involve atoms with positive spin densities, relatively strong intermolecular antiferromagnetic interactions, as well as electrical conductivity, are anticipated in crystalline diradical **4**.[2,11]

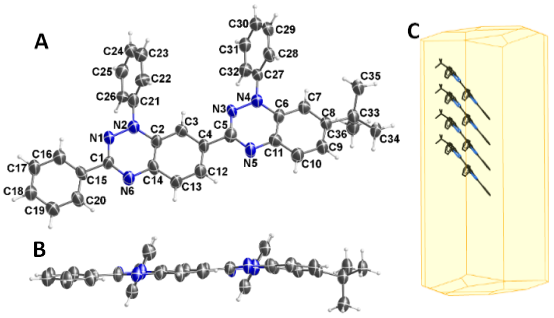


**Figure 2.** Single crystal X-ray structure of diradical **4** at 100 K, with carbon and nitrogen atoms depicted using thermal ellipsoids set at the 50% probability level (A and B). BFDH crystal morphoplogy (C). Additional data, e.g., for radical **10**, can be found in the SI: Figs. S1-S6 and Tables S1-S6.

EPR spectra of diradical **4** in a frozen glass at 110 K indicate a significant population of the triplet state. The forbidden $|\Delta m_s| = 2$ transition is relatively intense, which is consistent with a large spectral width ($2D = 782$ MHz) of the $|\Delta m_s| = 1$ region (Figure 3 and Table 1). *D*- and *g*-tensor orientations for **1**, **2**, and **4** are similar and the absolute values are well reproduced by DFT-computations for two major conformers, **4**A and **4**B, of **4**, except for the inherently difficult to compute parameter *E*.

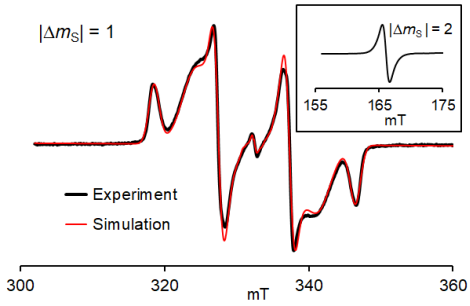


**Figure 3.** EPR (110 K, ν = 9.3269 GHz) spectrum for 0.54 mM diradical **4** in toluene/chloroform, 3:1 glass; a small center peak corresponds to monoradical impurity (ca. 5 – 7%). Inset: the $|\Delta m_s| = 2$ transition. Spectral simulation of the $|\Delta m_s| = 1$ region (rmsd = 0.0197, see: Table 1 and Fig. S15, SI.

We employ EPR spectroscopy to determine the triplet ground state of **4** in toluene/chloroform (4:1) by measurement of $\chi T$,

**Table 1. EPR parameters for triplet states of diradicals.**

| Diradicals | *D* (MHz) | *E* (MHz) | $g_x$ | $g_y$ | $g_z$ | $g_{iso}$[a] |
|---|---|---|---|---|---|---|
| **1** | 69.6 | 4.2 | 2.0069 | 2.0010 | 2.0052 | 2.0044 |
| **2** | 242 | 35.1 | 2.0072 | 2.0026 | 2.0052 | 2.0050 |
| **3** | ca. 75 | na | na | na | na | na |
| *o*-DBT | 126 | 39 | na | na | na | na |
| **4** | 391 | 35.9 | 2.0042 | 2.0027 | 2.0041 | 2.0037 |
| **4**A[b] | 406 | 71 | 2.0043 | 2.0023 | 2.0041 | 2.0036 |
| **4**B[b] | 410 | 60 | 2.0042 | 2.0022 | 2.0042 | 2.0036 |

[a] $g_{iso} \approx (g_x + g_y + g_z)/3$. [b] Computed with ORCA, SI, Table S9.[14]

the product of paramagnetic susceptibility ($\chi$) and temperature ($T$), in the $T$ = 110 – 331 K range. The spectra are acquired at each $T$ at least in triplicate and Tempone in the same solvent is used as a spin counting reference. The numerical fit of $\chi T$ vs. $T$ to the modified Bleaney-Bowers-like equation (eq. S2, SI)[2,15] suggests the presence of two equilibrating conformations **4**A and **4**B with singlet-triplet energy gaps $2J_A/k$ = 220 ± 70 K and $2J_B/k$ = –340 ± 37 K i.e., $\Delta E_{ST} \approx 0.4$ kcal mol$^{-1}$ for the major conformation **4**A (Figure 4).

Similarly, we study EPR double integrated intensities ($DI$) vs $T$ for polycrystalline **4**. Notably, a curved plot is obtained in the $T$ = 110 – 280 K range, with a broad maximum slightly above 200 K, rather than the usual $DI \sim 1/T$ paramagnetic behavior. In conjunction with the X-ray-determined crystal packing of **4**, suggesting formation of $S$ = 1 antiferromagnetic π-stacked 1-D chains of diradicals, the $DI$ vs $T$ data are fit to a 1-D chain model (SI, eq. S3A)[2,16] with two variable parameters, exchange coupling constant, $J'/k$ = –157 ± 3 K (mean ± SE), and conversion factor, $N$, of $DI$ to molar paramagnetic susceptibility $\chi$. Because of the Dysonian line shape for solid **4** (Figure 4),[17ac] $J'/k$ = –157 ± 3 K should be viewed as an order of magnitude estimate. A similar Dysonian line shape is obtained for a crystalline plate of **4** (5 × 2.5 × 0.13 mm$^3$) with angle-dependent $A/B$ =1.6–1.8 at $T$ = 294 K and polycrystalline **4** (particle size of <75 μm) with $A/B$ =1.5–1.9 at $T$ = 110–279 K. These results suggest that at 9 GHz, the skin depth, $\delta_c$, of solid **4** is of the order of 0.1 mm, which would imply comparable conductivity to $\sigma$ = 8.8 S cm$^{-1}$ for HOPG plates (4 × 0.4 × 0.2 mm$^3$) with $\delta_c$ = 0.19 mm and $A/B \approx 1.8$.[17b]

Two-probe conductivity measurements, which due to contact resistance, may be viewed as lower bounds for actual $\sigma$, give $\sigma$ = 1 × 10$^{-4}$ and 0.01 S cm$^{-1}$ for **4** in spin-coated film and single crystals, respectively.

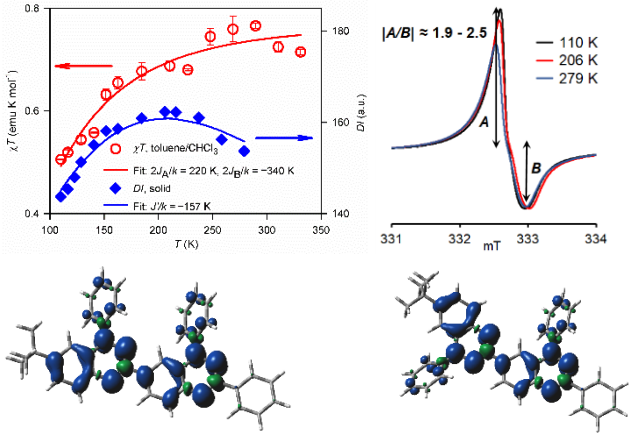


**Figure 4.** Top left: EPR spectroscopy of diradical **4**: plot and numerical fit of $\chi T$ vs $T$ in toluene/chloroform (4:1) and $DI$ vs $T$ for polycrystalline **4**. Top right: representative EPR spectra with Dysonian line shape for solid **4**. Further details are reported in the SI: Table S7, Figs. S13–S26, Eqs. S2 and S3A. Bottom: Spin density plots for triplet states of conformations **4**A and **4**B.

As suggested by the EPR-derived $\chi T$ vs. $T$ data and illustrated by spin density plots (Figure 4), the diradical **4** may exist in two major conformations **4**A and **4**B. Conformation **4**A corresponds to the one found in crystalline **4** (Figure 2). DFT computations at the UB3LYP/6-31G(d,p)+ZPVE level[18] suggest that triplet states of **4**A and **4**B are approximately isoenergetic. $\Delta E_{ST}$ values for **4**A and **4**B are surprisingly different, 1.37 and 0.34 kcal mol$^{-1}$, respectively; in addition, $J'/k \approx -100$ K is computed in the π-dimer at the X-ray geometry (SI, Tables S8 and S10). Because this level of theory is well-known to overestimate the stability of high-spin states,[1,2,19] it is possible that actual $\Delta E_{ST}$ for **4**B is negative, as determined experimentally (Figure 4).

TGA, with parallel IR spectroscopy, of diradical **4** indicates that the onset of decomposition is at $T$ > 264 °C, which is more than ~100 °C higher than recently studied $S$ = 1 diradical **2** (Figure 5).[2] Relying on this result, we deposit thin films of diradical **4** on $SiO_2$/Si(111) wafers by controlled evaporation under ultra-high vacuum (UHV). Following a well-established method,[4,20] we use X-ray photoelectron spectroscopy (XPS) together with a best fit procedure to assess the intactness and the stability of the diradical in the thin films. The XPS investigation indicate that the films have the expected stoichiometry (Figure 5), i.e., the evaporation of intact radicals was successfully achieved. This is further supported by the direct comparison with the XPS spectra of the powder that did not undergo evaporation and EPR spectroscopy (SI). The films grow following a strong island mode, as seen by atomic force microscopy (AFM, see: SI), indicating a strong interaction between molecules, and very weak interaction with the substrate.

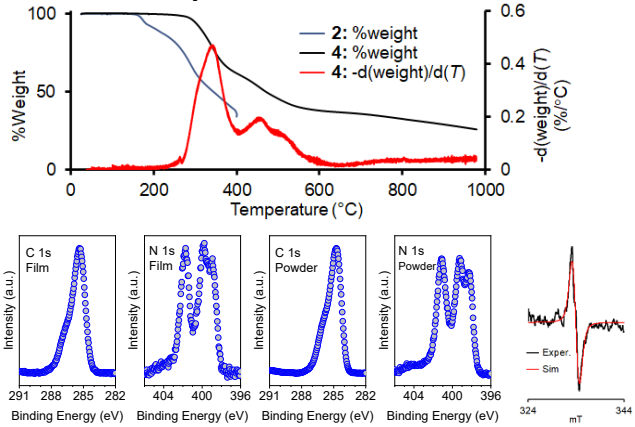


**Figure 5**. Top: Thermogravimetric analysis with IR spectra of diradicals **2** and **4** under $N_2$;[2] heating rate = 5 °C min$^{-1}$. For further details, including IR spectra, see: SI, Figs. S7 and S8. Bottom four left panels: C 1s and N 1s core level XPS spectra of a multilayer of **4** deposited on $SiO_2$/Si(111) substrate, compared to the powder spectra. Bottom right: preliminary EPR difference spectrum for thin film of **4** at 294 K showing Voigtian line shape with Lorentzian and Gaussian peak-to-peak linewidth of 0.6 and 1.3 mT, respectively. For further details, see: SI, Figs. S27–S37.

The EPR spectrum of nm-thick film of **4** shows a single isotropic peak with a line-shape intermediate between Gaussian and Lorentzian, thus suggesting conductance or exchange coupling in 1-D.[17c,21]

In conclusion, we have prepared the first high-spin ($S$ = 1) diradical, based entirely on two Blatter radical moieties, to attain the robust thermal stability. The crystalline diradical **4** displays good electrical conductivity, observed for the first time in a high-spin diradical. The diradical is evaporated under UHV to form thin films on silicon, which are relatively stable under vacuum (many days) or under air (at least 18 h).

## ASSOCIATED CONTENT

### Supporting Information

Complete acknowledgment and ref 18, general procedures and materials, additional experimental and computational details. This material is available free of charge via the Internet at http://pubs.acs.org.

## AUTHOR INFORMATION

* Corresponding Authors
arajca1@unl.edu and benedetta.casu@uni-tuebingen.de

### Notes

The authors declare no competing financial interests.

## ACKNOWLEDGMENT

We thank the NSF Chemistry Division for support of this research under Grants CHE-1665256 and CHE-1955349. Support for the acquisition of the Bruker Venture D8 diffractometer through the Major Scientific Research Equipment Fund from the President of Indiana University and the Office of the Vice President for Research is gratefully acknowledged. Financial support from the German Research Foundation (DFG) under the contract CA852/11-1 is gratefully acknowledged. We thank Prof. Letian Dou (Chemical Engineering at Purdue) for the design of the mask for the single crystal measurements of electrical conductivity.

REFERENCES

(1) Gallagher, N. M.; Bauer, J. J.; Pink, M.; Rajca, S.; Rajca, A. High-Spin Organic Diradical with Robust Stability. *J. Am. Chem. Soc.* **2016**, *138*, 9377–9380.

(2) Gallagher, N.; Zhang, H.; Junghoefer, T.; Giangrisostomi, E.; Ovsyannikov, R.; Pink, M.; Rajca, S.; Casu, M. B.; Rajca, A. Thermally and Magnetically Robust Triplet Ground State Diradical. *J. Am. Chem. Soc.* **2019**, *141*, 4764–4774.

(3) (a) Blatter; H. M.; Lukaszewski, H. A new stable free radical. *Tetrahedron Lett.* **1968**, *9*, 22, 2701–2705. (b) Constantinides, C. P.; Koutentis, P. A.; Krassos, H.; Rawson, J. M.; Tasiopoulos, A. J. Characterization and Magnetic Properties of a "Super Stable" Radical 1,3-Diphenyl-7-trifluoromethyl-1,4-dihydro-1,2,4-benzotriazin-4-yl. *J. Org. Chem*. **2011**, 76, 2798– 2806. (c) Zheng, Y.; Miao, M.-S.; Kemei, M. C.; Seshadri, R.; Wudl, F. The Pyreno-Triazinyl Radical – Magnetic and Sensor Properties. *Isr. J. Chem*. **2014**, *54*, 774–778. (d) Ciccullo, F.; Gallagher, N. M.; Geladari, O.; Chasse, T.; Rajca, A.; Casu, M. D. A Derivative of the Blatter Radical as a Potential Metal-Free Magnet for Stable Thin Films and Interfaces. *ACS Appl. Mater. Interfaces* **2016**, *8*, 1805–1812.

(4) Casu, M. B., Nanoscale studies of organic radicals: Surface, interface, and spinterface, *Acc. Chem. Res.* **2018**, *51*, 753–760.

(5) (a) Hutchison, K.; Srdanov, G.; Hicks, R.; Yu, H.; Wudl, F. Tetraphenylhexaazaanthracene: A Case for Dominance of Cyanine Ion Stabilization Overwhelming 16π Antiaromaticity. *J. Am. Chem. Soc.* **1998**, *120*, 2989–2990. (b) Constantinides, C. P.; Zissimou, G. A.; Berezin, A. A.; Ioannou, T. A.; Manoli, M.; Tsokkou, D.; Theodorou, E.; Hayes, S. C.; Koutentis, P. A. Tetraphenylhexaazaanthracenes: 16π Weakly Antiaromatic Species with Singlet Ground States. *Org. Lett.* **2015**, *17*, 4026– 4029. (c) Zheng, Y.; Miao, M.; Dantelle, G.; Eisenmenger, N. D.; Wu, G.; Yavuz, I.; Chabinyc, M. L.; Houk, K. N.; Wudl, F. A Solid-State Effect Responsible for an Organic Quintet State at Room Temperature and Ambient Pressure. *Adv. Mater.* **2015**, *27*, 1718–1723.

(6) (a) Hu, X.; Zhao, L.; Chen, H.; Ding, Y. Zheng, Y.-Z.; Miao, M.; Zheng, Y. Air stable high-spin blatter diradicals: non-Kekulé *versus* Kekulé structures. *J. Mater. Chem. C*, **2019**, *7*, 6559–6563. (b) Hu, X.; Chen, H.; Zhao, L.; Miao, M.; Han, J.; Wang, J.; Guo, J.; Hu, Y.; Zheng, Y. Nitrogen analogues of Chichibabin's and Müller's hydrocarbons with small singlet–triplet energy gaps. *Chem. Commun.* **2019**, *55*, 7812–7815. (c) Hu, X.; Chen, H.; Xue, G.; Zheng, Y. Correlation between the strength of conjugation and spin–spin interactions in stable diradicaloids. *J. Mater. Chem. C* **2020**, Adv. Article, published 03/25/2020. https://doi.org/10.1039/D0TC00868K

(7) (a) Ovchinnikov, A. A. Multiplicity of the ground state of large alternant organic molecules with conjugated bonds. *Theor. Chim. Acta.* **1978**, *47*, 297–304. (b) Gallagher, N. M.; Olankitwanit, A.; Rajca, A. High-Spin Organic Molecules. *J. Org. Chem.* **2015**, *80*, 1291–1298.

(8) (a) Rajca, A.; Rajca, S. Intramolecular Antiferromagnetic vs Ferromagnetic Spin Coupling Through the Biphenyl Unit. *J. Am. Chem. Soc.* **1996**, *118*, 8121–8126. (b) A. Rajca, J. Wongsriratanakul, S. Rajca, S. High-Spin Organic Polyradicals as Spin Clusters: Ferromagnetic Spin Coupling through Biphenyl Unit in Polyarylmethyl Tri-, Penta-, Hepta-, and Hexadecaradicals. *J. Am. Chem. Soc*. **1997**, *119*, 11674–11686.

(9) Shultz, D. A.; Fico, R. M., Jr.; Lee, H.; Kampf, J. W.; Kirschbaum, K.; Pinkerton, A. A.; Boyle, P. D. Mechanisms of Exchange Modulation in Trimethylenemethane-type Biradicals: The Roles of Conformation and Spin Density. *J. Am. Chem. Soc.* **2003**, *125*, 15426–15432.

(10) Joo, Y.; Agarkar, V.; Sung, S. H.; Savoie, B. M.; Boudouris, B. W. A nonconjugated radical polymer glass with high electrical conductivity. *Science* **2018**, *359*, 1391–1395,

(11) (a) Mailman, A.; Wong, J. W. L.; Winter, S. M.; Claridge, R. C. M.; Robertson, C. M.; Assoud, A.; Yong, W.; Steven, E.; Dube, P. A.; Tse, J. S.; Desgreniers, S.; Secco, R. A.; Oakley, R. T. Fine tuning the performance of multiorbital radical conductors by substituent effects. *J. Am. Chem. Soc.* **2017**, *139*, 1625–1635. (b) Pal, S. K.; Itkis, M. E.; Tham, F. S.; Reed, R. W.; Oakley, R. T.; Haddon, R. C. Resonating valence-bond ground state in a phenalenyl-based neutral radical conductor. *Science* **2005**, *309*, 281– 284.

(12) The mechanism for ring contraction to **10** is under investigation.

(13) The dihedral angle is between the C1-N1-N2-C2-C3-C4-C12-C13-C14-N6 and C5-N3-N4-C6-C7-C8-C8-C9-C10-C11-N5 planes.

(14) Neese, F. The ORCA program system. *Wiley Interdisciplinary Reviews: Comp. Mol. Sci.* **2012**, *2*, 73–78.

(15) (a) Rajca, A. Organic diradicals and polyradicals: from spin coupling to magnetism? *Chem. Rev.* **1994**, *94*, 871–893. (b) Shu, C.; Zhang, H.; Olankitwanit, A.; Rajca, S.; Rajca, A. High-Spin Diradical Dication of Chiral π-Conjugated Double Helical Molecule. *J. Am. Chem. Soc.*, **2019**, *141*, 17287–17294.

(16) Meyer, A.; Gleizes, A.; Girerd, J. J.; Verdaguer, M.; Kahn, O. Crystal structures, magnetic anisotropy properties, and orbital interactions in catena - (μ-nitrito) - bis (ethylenediamine) nickel(II) perchlorate and triiodide. *Inorg. Chem.* **1982**, *21*, 1729–1739.

(17) (a) Dyson, F. J. Electron Spin Resonance Absorption in Metals. II. Theory of Electron Diffusion and the Skin Effect. *Phys. Rev.* **1958**, *98*, 349–359. (b) Ziatdinov, A. M.; Skrylnik, P. G. Graphite intercalation by nitric acid: conduction ESR and theoretical studies. *Chem. Phys.* **2000**, *261*, 439–448. (b) Krinichnyi, V. I. Dynamics of spin charge carriers in polyaniline. *Appl. Phys. Rev.* **2014**, *1*, 021305.

(18) Frisch, M. J.; et al, *Gaussian 16*, Revision A.1 (Gaussian, Inc., Wallingford CT, 2016).

(19) Bajaj, A.; Ali, Md. E. First-Principle Design of Blatter's Diradicals with Strong Ferromagnetic Exchange Interactions. *J. Phys. Chem. C* **2019**, *123*, 15186–15194.

(20) Savu, S.-A.; Biswas, I.; Sorace, L.; Mannini, M.; Rovai, D.; Caneschi, A.; Chassé, T.; Casu, M. B., Nanoscale Assembly of Paramagnetic Organic Radicals on Au(111) Single Crystals. *Chem.-Eur. J.* **2013,** *19*, 3445–3450.

(21) Hennessy, M. J.; McElwee, C. D.; Richards, P. M. Effect of interchain coupling on electron-spin resonance in nearly one-dimensional systems. *Phys. Rev. B* **1973**, *7*, 930–947.

Insert Table of Contents artwork here